



JOURNAL OF LIMNOLOGY

DOI: 10.4081/jlimnol.2025.2192

SUPPLEMENTARY MATERIAL

Revisiting lakes within the Rideau Canal system (Ontario, Canada) to assess the impacts of multiple environmental stressors over the past ~25 years using diatom-based paleolimnology

Kapillesh Balasubramaniam,^{1*} Kathleen M. Rühland,¹ Andrew M. Paterson,²
John P. Smol¹

¹Paleoecological Environmental Assessment and Research Laboratory (PEARL),
Department of Biology, Queen's University, Kingston

²Environmental Monitoring and Reporting Branch, Ontario Ministry of Environment,
Conservation and Parks, Dorset, ON, Canada

*Corresponding author: 15kb63@queensu.ca

Key words: canal construction; climate warming; diatoms; eutrophication; shallow lakes; zebra mussels.

Tab. S1. The results of Spearman rank correlation analysis between MAAT trends and paleo-proxy (diatom and VRS-Chla) data. To integrate the diatom data with the MAAT data prior to correlation analysis, average air temperature during the period of accumulation for each sediment interval was calculated to account for the differences in temporal resolution between instrumental and sedimentary data. The boxes shaded in green indicate significant correlations ($p < 0.05$).

Parameter	Big Rideau L.	Indian L.	Upper Rideau L.	Lower Rideau L.	L. Opinicon	Otter L. (CR)
PC1	$p = 0.0012$; $\rho = 0.82$	$p = 0.001486$; $\rho = -0.7230392$	$p = 0.074$; $\rho = -0.46$	$p = 0.005$; $\rho = 0.63$	$p = 0.003981$; $\rho = 0.7582418$	$p = 2.2e-16$; $\rho = 0.8928571$
PC2	$p = 0.016$; $\rho = 0.68$	$p = 0.04904$; $\rho = -0.4877451$	$p = 0.018$; $\rho = -0.58$	$p = 0.1762$; $\rho = 0.333$	$p = 0.4043$; $\rho = 0.2527473$	$p = 0.9949$; $\rho = -0.0035714$
Small Benthic Fragilarioid Sum	$p = 0.0794$; $\rho = 0.53$	$p = 0.7155$; $\rho = -0.0955882$	$p = 0.126$; $\rho = 0.40$	$p = 0.008074$; $\rho = -0.603$	$p = 0.06416$; $\rho = -0.532967$	$p = 0.5844$; $\rho = 0.1537087$
Planktonic Sum	$p = 0.3593$; $\rho = 0.29$	$p = 0.01626$; $\rho = 0.5808824$	NA	$p = 0.0002$; $\rho = 0.7702$	$p = 0.007498$; $\rho = 0.7197802$	$p = 0.00108$; $\rho = 0.775$
<i>Aulacoseira</i> Sum	$p = 0.097$; $\rho = -0.50$	$p = 0.01331$; $\rho = -0.5955882$	$p = 0.0008$; $\rho = -0.75$	$p = 0.01597$; $\rho = -0.559$	$p = 0.2341$; $\rho = -0.3548834$	$p = 0.000674$; $\rho = -0.7928571$
Hill's N2	$p = 0.01902$; $\rho = 0.6619975$	$p = 0.9209$; $\rho = 0.02696078$	$p = 0.4473$; $\rho = 0.20$	$p = 0.1243$; $\rho = 0.37584$	$p = 0.05813$; $\rho = 0.543956$	$p = 0.4819$; $\rho = -0.1964286$
VRS-Chla	$p = 0.001561$; $\rho = 0.8056054$	$p = 0.09752$; $\rho = 0.4166667$	$p = 0.0002$; $\rho = 0.80$	$p = 0.0006$; $\rho = 0.727$	$p = 0.3436$; $\rho = -0.2857143$	$p = 0.006525$; $\rho = 0.6821429$

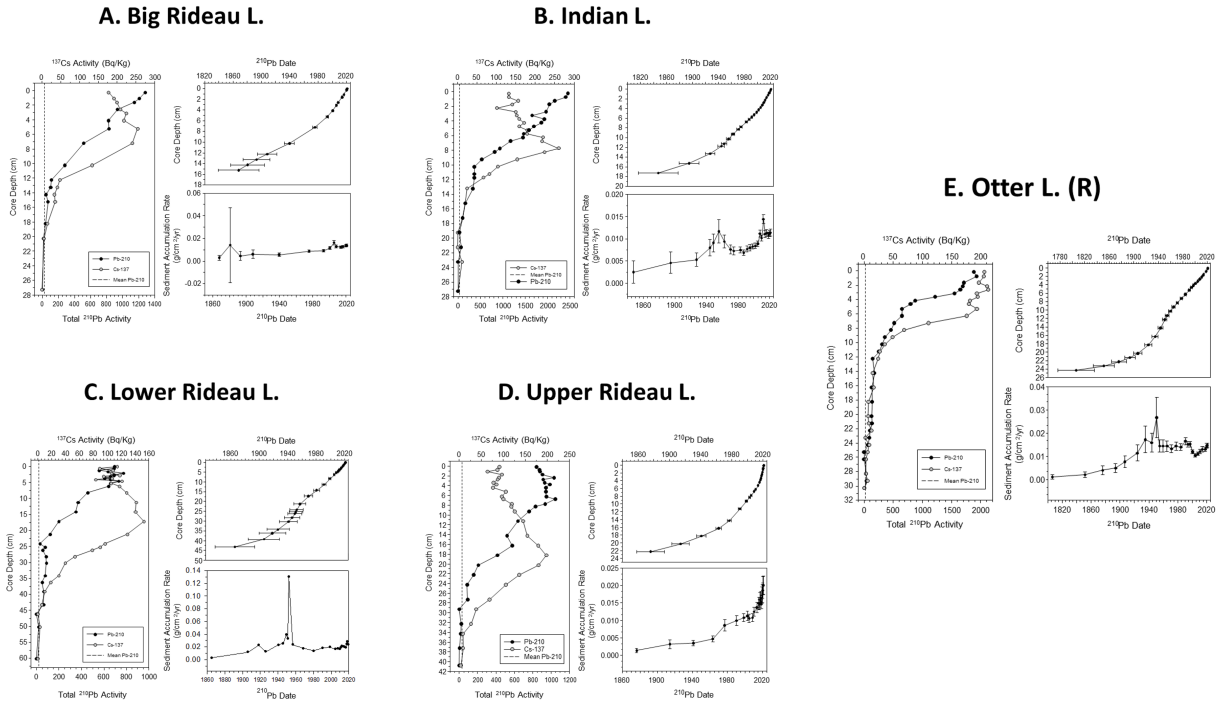


Fig. S1. Results of ^{210}Pb dating using gamma spectrometry for Big Rideau L. (A), Indian L. (B), Lower Rideau L. (C), Upper Rideau (D), and Otter L. (E). Gamma activities for ^{210}Pb , ^{137}Cs , and mean ^{214}Pb (proxy for supported/background ^{210}Pb levels) were plotted against sediment core depth (right panels). Age-depth plots showing the estimated ^{210}Pb dates (with standard errors) derived from the constant rate of supply (CRS) model plotted against sediment core depth are shown in the upper left-hand panels. Sedimentation accumulation rates (with standard errors) based on CRS models were plotted against estimated ^{210}Pb dates and are shown in the lower left panels.

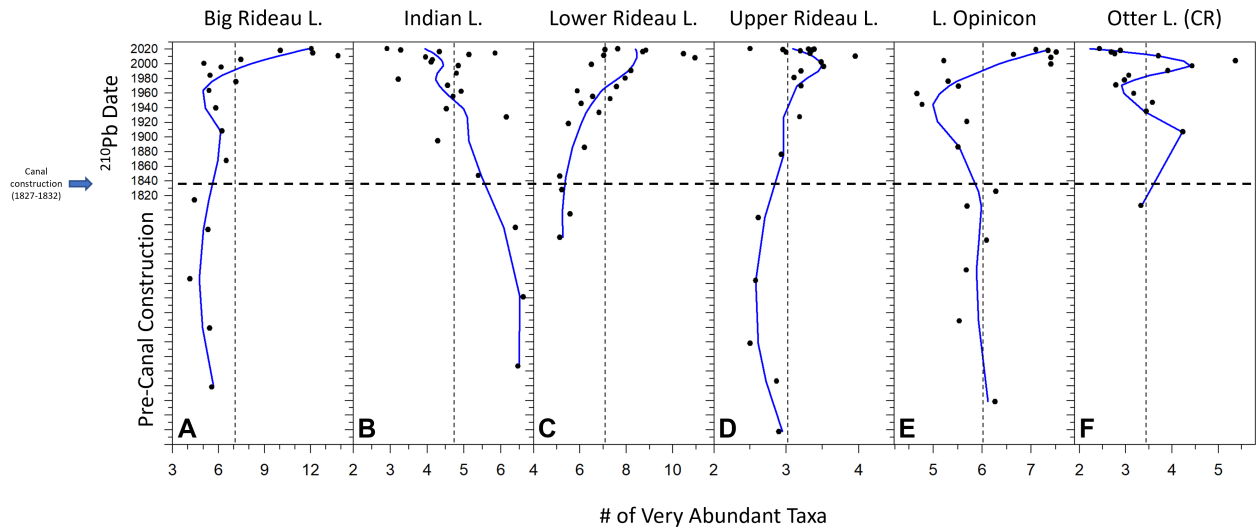


Fig. S2. Trends in Hill's N2 diversity index (plotted as the number of 'very abundant' taxa (*sensu* Birks, 2010), scaled by CRS-estimated ^{210}Pb dates for Big Rideau L. (A), Indian L. (B), Lower Rideau L. (C), Upper Rideau L. (D), L. Opinicon (E), and Otter L. (F). The vertical dashed lines represent the mean number of 'very abundant' taxa over the span of the record. Trends were highlighted using LOESS with a span of 0.8 (blue solid lines). The date of canal construction is highlighted with a blue arrow. Dates in bold and italicized font represent extrapolated age estimates that correspond to the construction of the Rideau Canal (~1830); these dates are viewed with caution as the associated errors are potentially high.

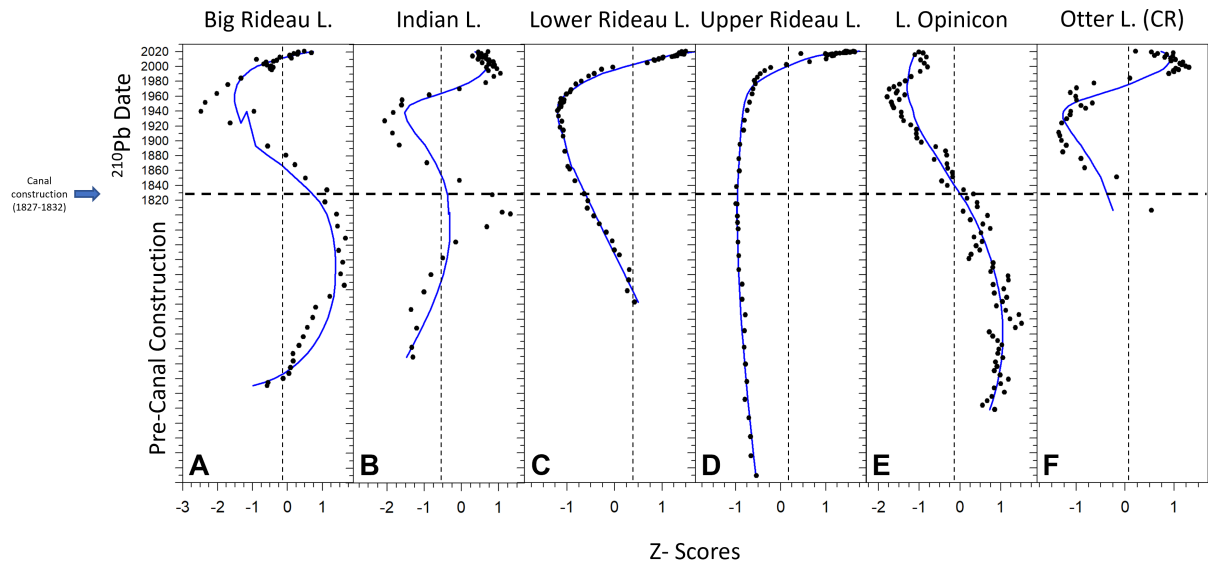


Fig. S3. Trends in visible range spectroscopy-inferred chlorophyll-*a* (VRS-Chla) concentrations (expressed as Z-scores) scaled by CRS-estimated ^{210}Pb dates for Big Rideau L. (**A**), Indian L. (**B**), Lower Rideau L. (**C**), Upper Rideau L. (**D**), L. Opinicon (**E**), and Otter L. (**F**). The vertical dashed lines represent the mean VRS-Chla concentrations over the span of the record. Trends in VRS-Chla were highlighted using LOESS with a span of 0.8 (blue solid lines). The horizontal dashed line and blue arrow depicts the date of canal construction. Dates in bold and italicized font represent extrapolated age estimates that correspond to the construction of the Rideau Canal (~1830); these dates are viewed with caution as the associated errors are potentially high.

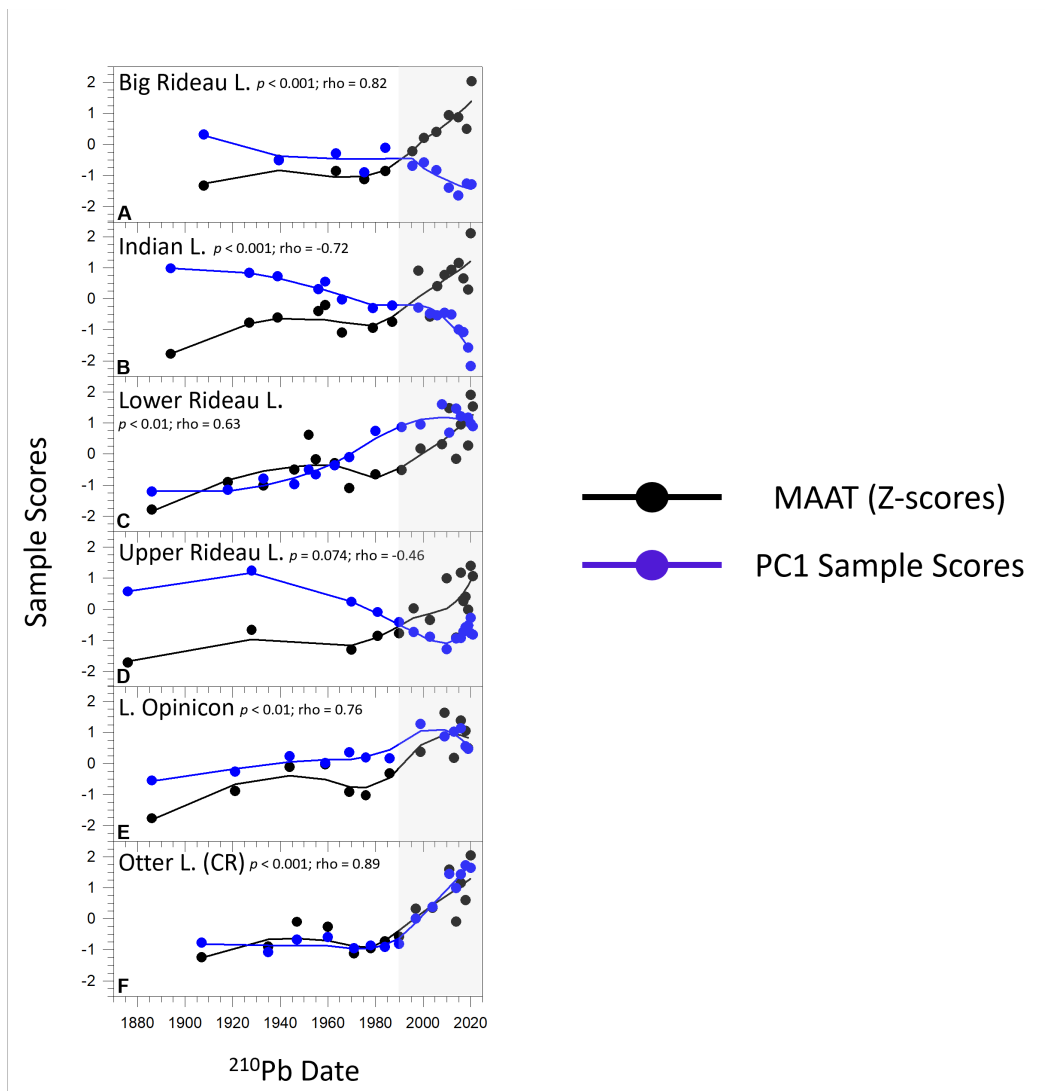


Fig. S4. Comparison between mean annual air temperature (MAAT) data (expressed as Z-scores and depicted by black symbols and lines) and principal component analysis (PCA) axis 1 sample scores (blue symbols and lines) for Big Rideau L. (A), Indian L. (B), Lower Rideau L. (C), Upper Rideau L. (D), L. Opinicon (E), and Otter L. (F). Included are the results of a Spearman rank correlation analysis. Prior to undertaking correlation analysis, the diatom and MAAT data were integrated by averaging the air temperature recorded during the period of accumulation for each sediment interval to account for the differences in temporal resolution between instrumental and sedimentary data. Shaded area depicts the post-1990 period (the period after the previous paleo studies were undertaken) focused on for this study and the period of greatest regional air temperature acceleration.